Scaling laws for liftoff velocity for wind-transported particles during particle–bed collisions

C. W. JIANG[1,2,3*], Z. C. ZHANG[3], Z. B. DONG[3], X. Y. WANG[1] and F. Jun. XIAO[3]

[1]Key Laboratory for Ecology and Environment of River Wetlands in Shaanxi Province, College of Environment and Life Sciences, Weinan Normal University, Weinan 714000, China

[2]Key Laboratory of Desert and Desertification, Northwest Institute of Eco-environment and Resources, Chinese Academy of Sciences, Lanzhou 730000, China

[3]School of Geography and Tourism, Shaanxi Normal University, Xi'an 710000, China

***Corresponding author:** Key Laboratory for Ecology and Environment of River Wetlands in Shaanxi Province, College of Environment and Life Sciences, Weinan Normal University, Middle section of Chaoyang Street, Weinan, Shaanxi Province 714000, China.

Tel./Fax: +86-913-213-3389. E-mail address: jiangchanwen@126.com

Abstract: We performed wind tunnel studies of sand–bed collisions with natural sand particles and found an impact angle of 10.5° over a loose bed, and calculated the critical impact velocity ($v_{ic} \cong 1.2027$ m s^{-1}). The number of splashing particles (N_s) increased linearly with v_i, but the coefficient of restitution *CoR* decreased linearly with v_i. The momentum lost through frictional processes α_{lost} was insensitive to v_i, with a value of 0.2466. The mean splash velocity increased with v_i for $v_i < 7$ m s^{-1}, and gradually reached its maximum value (0.7534 m s^{-1}) at $v_i = 7$ m s^{-1}, whereas $\bar{v}_s$ decreased slowly with v_i for $v_i > 7$ m s^{-1} and gradually approached a constant (0.6137 m s^{-1}). In addition, we developed a probability distribution model for liftoff velocity. Our results emphasize the crucial role of the impact angle and have significant consequences for modeling sand–bed collisions in a natural environment.

1. Introduction

The study of windblown sand started 80 years ago with Bagnold's (1941) seminal work. Bagnold was the first to propose that saltation is the main mode of sand transport. Collisions between saltating particles and the bed are key processes, as they reflect the interaction between these particles and the bed (Bagnold, 1941; Chepil, 1945; Owen, 1964; McKenna Neuman & Nickling, 1994). These interactions are usually described by splash functions, which describe the relationships between the velocities and angles of the incident particles and related post-collision parameters such as the number of splashed particles and the velocity and angle of the splashed and rebounding particles (Ungar & Haff, 1987). Both theoretical models and experiments have shown that the splash functions are very sensitive to the impact angle, and due to the action of the airflow above a bed, the impact angle of sand particles on a flat surface is about 10° (Anderson & Haff, 1991; Dong et al., 2002; Cheng et al., 2006; Gordon & McKenna Neuman, 2009; Chen et al., 2019; Zhang et al., 2022). Surprisingly, few measurements of these collisions have been obtained with impacts around this typical impact angle (Gordon & McKenna Neuman, 2009). This may be due to the difficulty of obtaining data in the field and wind tunnel with a high particle density (Gordon & McKenna Neuman, 2009; Chen et al., 2019).

Because the collision occurs inside the near-surface boundary layer, the effect of air

flow during a collision is negligible (Haff & Anderson, 1988, 1991). Many scholars have obtained splash functions by conducting particle–bed collision experiments without wind by using devices to launch the particles (Rioual et al., 2000, 2003; Beladjine et al., 2007; Chen et al., 2019; Zhang et al., 2022). The most typical launch devices are launch guns and centrifugal launchers. However, launch guns can only launch materials with a larger than natural particle size (d > 4 mm) that substitute for much smaller natural particles, and the airflow generated in the gun barrel would alter the characteristics of the impact when they use this device to launch natural sand particles ($d \cong 0.25$ mm) (Mitha et al., 1986; Rioual et al., 2000, 2003; Beladjine et al., 2007). Because the splash functions are very sensitive to the density and Young's modulus (deformability) of the material, launch gun experiments cannot reflect the characteristics of natural sand transport well. Although centrifugal launchers can launch natural sand particles without generating a disruptive airflow, it is difficult to achieve an impact angle below 20°, which is much greater than the actual angle during natural sand transport (Chen et al., 2019; Zhang et al., 2022). Because splash functions are very sensitive to the impact angle, the resulting data don't reflect natural impact processes. Therefore, it is difficult to obtain accurate splash functions for natural sand with a more realistic impact angle of about 10° based on experiments with too-large particles and without wind.

In this letter, we describe experimental evidence obtained through careful wind tunnel measurements of collisions between saltating particles and a loose bed of natural sand. We calculated the critical impact velocity ($v_{ic} \cong 1.2027 \pm 0.0791$ m s^{-1}) for aeolian sand flow in air for the first time at an impact angle of 10°, and found that the splash functions for sand particles with this impact angle differ quantitatively from those in previous research obtained using substitute materials with a larger particle size or natural sand with a larger impact angle (Beladjine et al., 2007; Chen et al., 2019). However, our results support the conclusion of Ho et al. (2011) that increasing v_i will lead to more splashing of particles and have less impact on the liftoff velocity (v_L). Using our results, we developed a more realistic probability distribution model for v_L based on the distributions of v_r and v_s. Our results emphasize the critical role of the impact angle in the interactions between saltating aeolian sand particles and an erodible bed.

2. Wind tunnel experiment

Our experiment was conducted in the wind tunnel of the Northwest Institute of Eco-Environment Resources, Chinese Academy of Sciences, which has a total length of 10.5 m and a range of axial wind speeds from 1.0 m s^{-1} to 35.0 m s^{-1} (Jiang et al., 2022). The test section (4 m long, 0.4 m tall, and 0.4 m wide) was covered by a 1-cm-thick sample of dry natural sand with a range of grain sizes (hereafter, sand sample G_1). Before each trial, it was gently leveled with a wooden ruler. The experimental sand samples and corresponding wind conditions are shown in Table 1. We recorded a total of 749 particle–bed collision events and divided them into five grades according to the number of splashed particles (N_s = 0, 1, 2, 3, or 4) by a high-speed camera with a Micro lens (see Fig. 1). The corresponding numbers of collision events were 596, 121, 24, 6, and 2, respectively. Relevant parameters during collision events (i.e., the angles and velocities of impact particles, rebounding

particles, and splashing particles) were determined by means of particle-tracking velocimetry (Jiang et al., 2022). The average impact angle during the 749 collision events was 10.5° and the standard deviation was 4.5°. Their incidence velocity (v_i) ranged from 0.5 to 5.0 m s^{-1}.

Table 1 Experimental conditions: d is the particle diameter. u_* is the wind shear velocity. G_1 was a natural desert sand from Tengger Desert in northern China, and G_2 to G_7 were artificial quartz sands with good roundness (glass microbeads), which had a basic density ($\rho \cong 2650$ kg m^{-3}) similar to that of the typical natural sand (Bagnold, 1941). h, $v_{ic} / [gd]^{0.5}$, and v_{ic}/u_* are the regression parameters in equation 1 for the seven sand samples. All regressions were significant at $P < 0.05$.

Sample	d (mm)	u_* (m s^{-1})	h	v_{ic}	$v_{ic}/ [gd]^{0.5}$	v_{ic}/u_*	R^2
G_1	0.10–0.12	0.25	1.4568	1.2348	37.6088	4.9392	0.9959
G_2	0.1–0.2	0.26	1.5039	1.2421	32.3692	4.7773	0.9956
G_3	0.2–0.3	0.28	1.4461	1.1270	22.7683	4.0249	0.9769
G_4	0.3–0.4	0.31	1.6807	1.0736	18.3307	3.4631	0.9710
G_5	0.4–0.5	0.33	1.4912	1.2151	18.2969	3.6820	0.8854
G_6	0.6–0.7	0.45	1.5602	1.2125	15.1912	2.6943	0.8702
G_7	0.7–0.8	0.49	1.1968	1.3136	15.3223	2.6809	0.9916

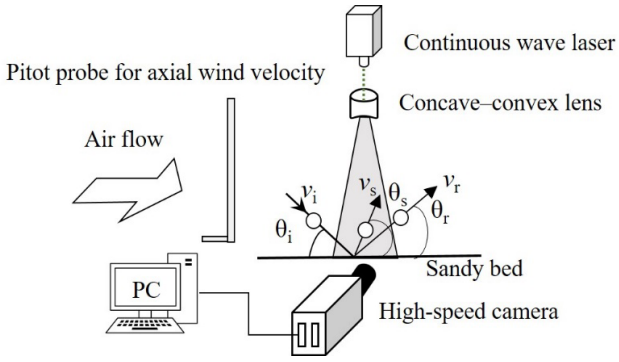

Figure 1. Experimental layout and definition of the measured collision parameters. v_i and θ_i are the velocity and angle of the incident particles, respectively. v_r and θ_r are the velocity and angle of the rebounding particles, respectively. v_s and θ_s are the velocity and angle of the splashing particles, respectively.

3. Results

3.1. Number of splashed particles

N_s increased linearly with increasing v_i (Fig. 2A), and satisfied the equation form proposed by Beladjine et al. (2007):

$$N_s = h\left(\frac{v_i}{v_{ic}} - 1\right) \quad (1)$$

where h is a function of the impact angle, v_i is the impact velocity (m s^{-1}), and v_{ic} is

the critical impact velocity (m s^{-1}) at which splashing begins (Beladjine et al., 2007).

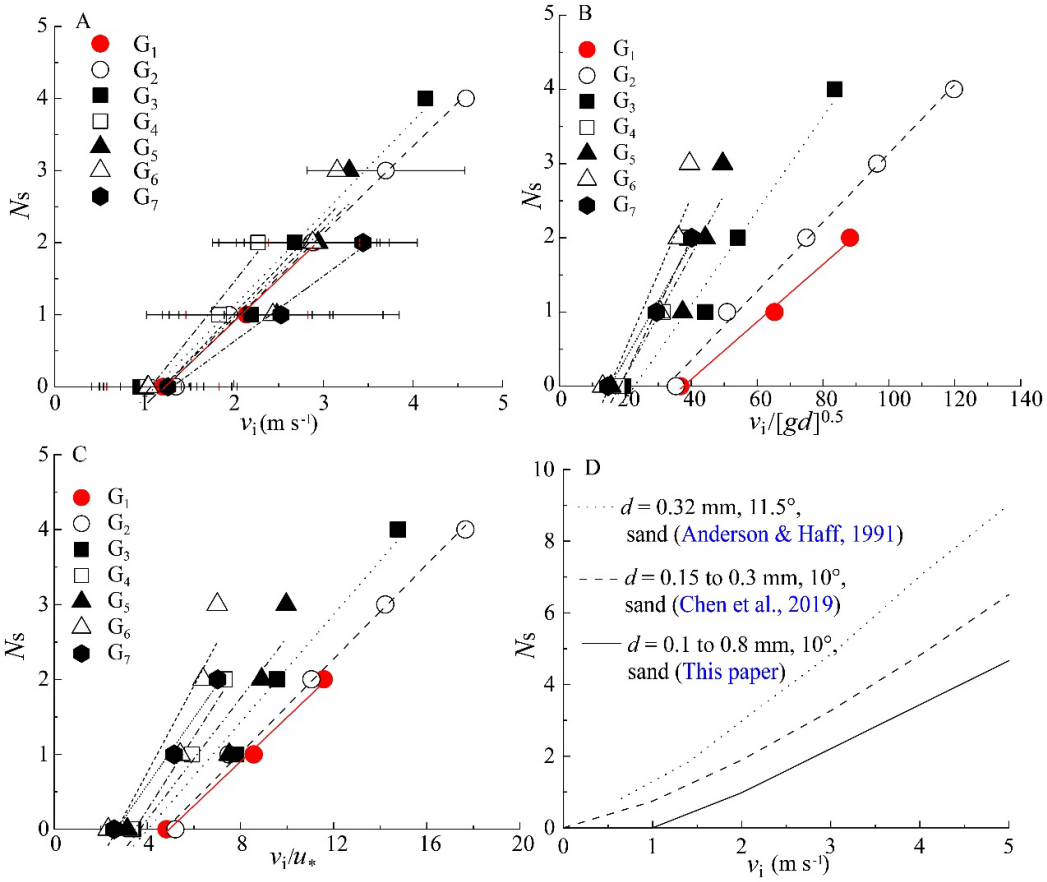

Figure 2. Relationship between the number of splashed particles (N_s) and the impact velocity (v_i) (A) and v_i standardized with respect to particle size (v_i / $[gd]^{0.5}$) (B) and v_i standardized with respect to the shear velocity (v_i / u_*) (C). Table 1 contains the regression parameters (h, v_{ic}/ $[gd]^{0.5}$, and v_{ic}/u_* in equation 1) for the seven sand samples. (D) Relationship between N_s and v_i in the present study and two previous studies.

To the best of our knowledge, v_{ic} has been ignored by researchers (Anderson & Haff, 1991; Chen et al., 2019). This has made it difficult to determine the critical v_L for sand particles based on their liftoff height in collision experiments without a wind (Beladjine et al., 2007). Based on the data in Figure 2A, we calculated v_{ic} for aeolian sand flow in air for the first time, and found that $v_{ic} \cong 1.2027 \pm 0.0791$ m s^{-1}, as shown in Table 1 with h at an impact angle of 10° = 1.4765 ± 0.1468. The absolute incident velocity graphs (Fig. 2A) collapse well, while a comparable data collapse could not be obtained for the rescaled distributions (Fig. 2B and Fig. 2C). Thus, N_s appears to be relatively independent of the particle size (d) and wind strength (u_*).

Our results are obviously lower than the results of Chen et al.'s (2019) centrifugal particle launcher experiment and those in Anderson & Haff's (1991) theoretical model (Fig. 2D). The impact angles reported by Chen et al. (2019) ranged from 20° to 48°; the dashed curve in Figure 2D results from substituting the impact angle θ_i into

equation 9 in Chen et al. (2019). The relationship between N_s and v_i also differed greatly from that in studies that used large particles as substitute materials, such as Beladjine et al. (2007), who used PVC beads (d = 6 mm) and obtained h (at 10°) ≅ 5.4 and found that v_{ic} ≅ 9.7 m s^{-1} for θ_i = 10°.

3.2. Coefficient of restitution and Splash velocity

The coefficient of restitution, $CoR = v_r / v_i$, represents the proportion of the momentum of the saltating particle that is retained when it rebounds (Zhang et al., 2022). CoR decreased linearly with increasing N_s (Fig. 3A). The equation for the probability distribution of rebound velocity proposed by Anderson & Haff (1991) was $P_r = 0.95(1 - \exp[-\gamma v_i])$, where P_r is the rebound probability and γ = 2 m s^{-1}, and mainly suggests the probability that particles with a low momentum (v_i < 2 m s^{-1}) are unlikely to rebound after a collision. In the present study, our impact velocities reached about 5 m s^{-1}, and if we extrapolate the graph to N_s = 7, we find that CoR ≅ 0, which suggests that the impacting particles will be completely captured by the loose bed surface if v_i > 7 m s^{-1}. We can express this relationship as follows:

$$CoR = \begin{cases} -0.1006N_s + 0.7212, & N_s \le 7 \\ 0, & N_s > 7 \end{cases} \quad (2)$$

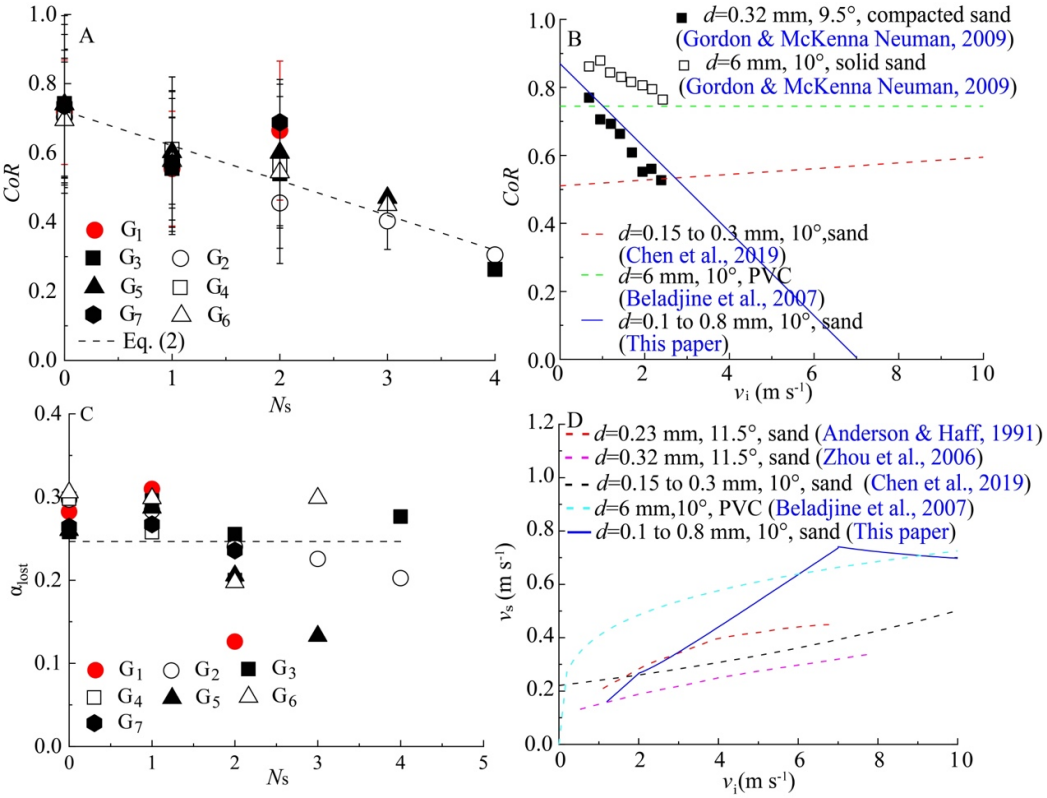

Figure 3. Relationships between the coefficient of restitution (CoR) and the (A) number of splashed particles (N_s) and (B) impact velocity (v_i). (C) Relationship between the frictional momentum loss fraction (α_{lost}) and the number of splashed particles (N_s). (D) The relationship between the splash velocity (v_s) and the incidence velocity (v_i).

By combining equations 1 and 2, we can obtain the relationship between CoR and v_i:

$$CoR \cong \begin{cases} -0.1235v_i + 0.8697, & v_i \leq 7.0\ m/s \\ 0, & v_i > 7.0\ m/s \end{cases} \quad (3)$$

The relationship between CoR and v_i is highly controversial. Beladjine et al. (2007) studied this relationship using PVC particles (d = 6 mm) and found (Fig. 3B, green dotted line) that CoR was independent of v_i and negatively correlated with the sine of the impact angle ($CoR \cong 0.87 - 0.72 \sin \theta_i$, with θ_i expressed in radians). In contrast, Gordon & McKenna Neuman's (2009) wind tunnel results with a loose bed showed that CoR decreased linearly with increasing v_i (Fig. 3B, black solid squares). Experimental results with 5.9-mm plastic beads (Rioual et al., 2000) showed that CoR decreased slightly with increasing v_i. Chen et al. (2019) extrapolated their results from a large angle (20° to 48°) in an experiment without wind, and found that CoR increased linearly with increasing v_i when θ_i =10° and proposed that Gordon & McKenna Neuman's (2009) results may represent a special case under the condition of low v_i. However, our impact velocity reached about 5 m s^{-1} and our equation 3 described Gordon & McKenna Neuman's (2009) wind tunnel results well for a loose bed (Fig. 3B, blue solid line). These results suggest that CoR is sensitive to θ_i, particle density, Young's modulus for the material, and particle size. The grain size range (d = 0.1 to 0.8 mm) in our experiment covers most of the natural range of sand grain sizes and we found that CoR was insensitive to particle size and wind strength in this range (Fig. 3A). The basic density of the artificial quartz grains that we selected was close to that of natural sand, and Figure 3A also shows that the CoR results for natural sand with d = 0.10 to 0.12 mm were close to those with the artificial quartz particles of the same size. Thus, our experimental results were able to reflect the characteristics of natural sand.

According to our assumption of conservation of momentum in the collision process, the proportion of the momentum transferred to the splashed particles (α_s) can be expressed as:

$$\alpha_s = \frac{N_s \bar{v}_s}{v_i} = 1 - \alpha_{lost} - CoR \quad (4)$$

where $\alpha_{lost} = \frac{v_i - N_s \bar{v}_s - v_r}{v_i}$, and α_{lost} represents the momentum loss through frictional processes (Kok & Renno, 2009). $\bar{v}_s$ is the mean splash speed. α_{lost} ranges between 0.1 and 0.3 (Fig. 3C), and it was insensitive to N_s. This means that α_{lost} = 0.2466 ± 0.0351.

The expression for the mean splash velocity ($\bar{v}_s$) can be obtained by substituting α_{lost} into equation Eq. (4):

$$\bar{v}_s \cong \left(\frac{0.7534 - CoR}{N_s}\right) v_i \quad (5)$$

Based on equation (3), when v_i > 7.0 m s^{-1}, CoR = 0. Thus, $\bar{v}_s \cong 0.7534 v_i / N_s$ when v_i > 7.0 m s^{-1}. Moreover, $\bar{v}_s$ is only a realistic value if $N_s \geq 1$. Then, according to equation (1), if we assume that N_s = 1 and 1.2 < v_i < 2.0 m s^{-1}, $\bar{v}_s \cong 0.1328 v_i$ based on equations (2) and (5). Therefore, if we combine equations (1), (2) , (3), and (5), the relationship between $\bar{v}_s$ and v_i can be expressed as follows:

$$\bar{v}_s \approx \begin{cases} 0.1328 v_i & 1.2 \text{ m s}^{-1} < v_i < 2.0 \text{ m s}^{-1} \\ \frac{0.1235 v_i^2 - 0.1163 v_i}{1.2277 v_i - 1.4765} & 2.0 \text{ m s}^{-1} \le v_i \le 7.0 \text{ m s}^{-1} \\ \frac{0.7534 v_i}{1.2277 v_i - 1.4765} & v_i > 7.0 \text{ m s}^{-1} \end{cases} \quad (6)$$

In addition, $\lim_{v_i \to \infty} \frac{0.7534 v_i}{1.2277 v_i - 1.4765} = 0.6137$ m s^{-1}.

Equation (6) shows that when $v_i < 7.0$ m s^{-1}, $\bar{v}_s$ increases with increasing v_i, and the maximum splash velocity $\bar{v}_{s,max} \cong 0.7534$ m s^{-1} when $v_i \cong 7.0$ m s^{-1}. In contrast, when $v_i > 7.0$ m s^{-1}, $\bar{v}_s$ decreases with increasing v_i and gradually approaches a constant value of 0.6137 m s^{-1} (Fig. 3D, solid blue line).

In our results, v_s increased with increasing v_i and there was a threshold (maximum) v_i. This agrees with the results of Beladjine et al. (2007), who proposed that v_s is proportional to the 0.25 power of v_i (Fig. 3D), and the results of Anderson & Haff (1991), who proposed that v_s was proportional to the 0.30 power of v_i (Fig. 3D). However, our results differed from the model results of Zhou et al. (2006) (Fig. 3D) and the extrapolation result of Chen et al.'s (2019) windless experiment (Fig. 3D), which showed no obvious maximum boundaries, which is quite different from our results. Equations (1), (2) and (6) support the conclusion of Ho et al. (2011) that increasing v_i will lead to more splashing of particles and have less impact on the liftoff velocity (v_L) .

3.3. Probability distribution model of liftoff speed

The relationship between N_s and rebound angle (or splash angle) is not obvious (Fig. 4A and 4B). However, we can roughly estimate that the mean rebound angle was $\bar{\theta}_r \cong 32 \pm 11°$, and the mean splash angle was $\bar{\theta}_s \cong 34° \pm 15°$. Our rebound angles θ_r were similar to some previous results (Anderson & Haff's ,1991; Chen et al., 2019; Zhou et al., 2006; Xie, 2005). Therefore, when $\theta_i = 10°$, θ_r may be insensitive to the particle basic density, Young's modulus of the material, and v_i. However, our splash angles θ_s were lower than most previous windless results (Chen et al., 2019; Beladjine et al., 2007; Kok & Renno, 2009). We hypothesize that a major reason for the lower θ_s in our results is that the particles that lifted off at a large angle would have been quickly diverted by the airflow.

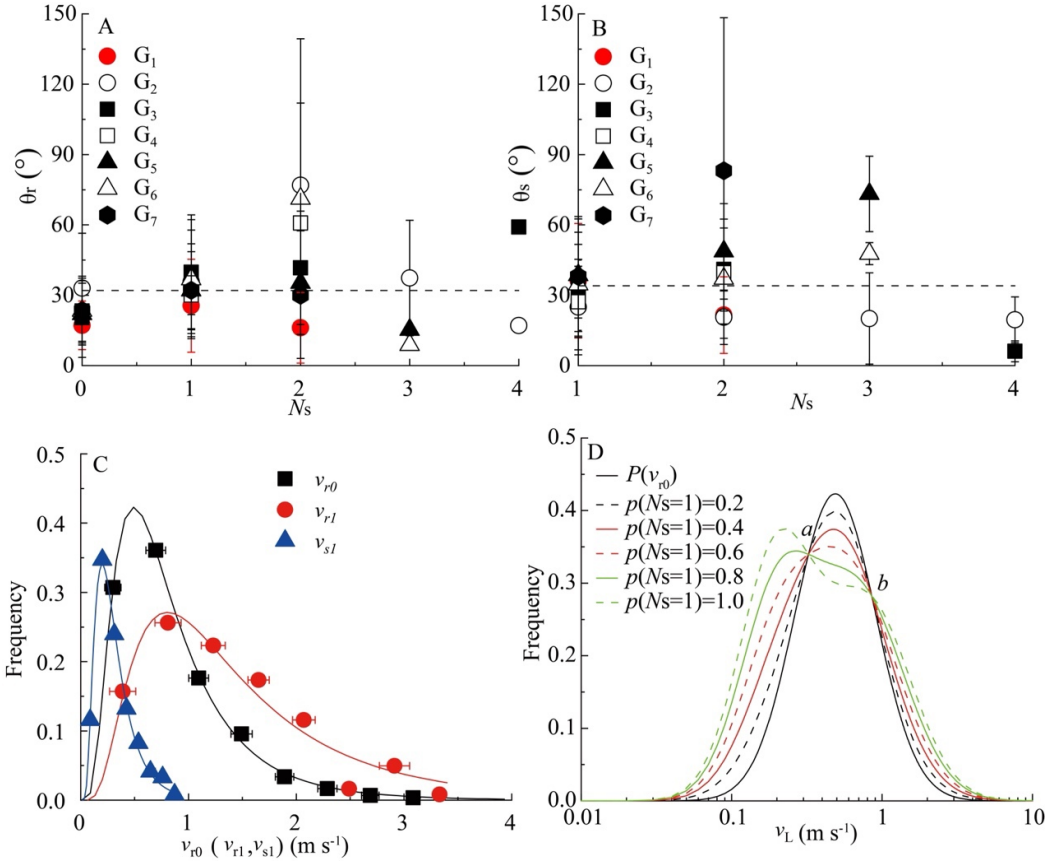

Figure 4. The relationships between the number of splashed particles (N_s) and (A) the rebound angle (θ_r) and (B) the splash angle (θ_s). Probability distributions of (C) rebound speed (v_r) and splash speed (v_s) for a number of splashed particles (N_s) of 0 and 1 during collision events and (D) liftoff velocity (v_L).

The present study showed that the liftoff of particles during a steady-state sand flow are mainly composed of rebounding and splashing particles provided by collision processes. Collisions with N_s values of 0 or 1 dominated the collision events. Thus, the probability distribution function for liftoff velocity, $P(v_L)$ can be expressed as follows:

$$P(v_L) = P(v_{s1})p(N_s = 1) + P(v_{r1})p(N_s = 1) + [1 - p(N_s = 1)]P(v_{r0}) \quad (7)$$

where $p(N_s) = 1$ is the occurrence probability of $N_s = 1$ collision event. $P(v_{s1})$, $P(v_{r1})$, and $P(v_{r0})$ are probability distribution functions for v_s of a collision event with $N_s = 1$, for v_r of a collision event with $N_s = 1$, and for v_r of a collision event with $N_s = 0$, respectively.

By combining data from the seven sand samples described in Table 1, we obtained relatively smooth probability distribution curves for rebound velocity and splash velocity. Both v_r and v_s were described by a log-normal distribution function (see Fig. 4C):

$$P(x) = A_0 \frac{\exp(-[\ln(x)-\lambda]^2/(2\delta^2))}{x} \quad (8)$$

where A_0, λ, and δ are fitting values, whose values are listed in Table 2.

Table 2 Fitting parameters for equation 8 for the number of splashed particles (N_s) of 0 and 1 for rebound velocity (v_{r0} and v_{r1}, respectively) and for splash velocity (v_{s1}). Graphs of the distributions are shown in Figure 4C.

Variable	A_0	λ	δ	R^2
v_{r0}	0.2508	–0.3310	0.6195	0.9984
v_{r1}	0.2712	0.2196	0.6618	0.9389
v_{s1}	0.0794	–1.2963	0.5648	0.9953

We examined the effects of setting $p(N_s = 1)$ to 0, 0.2, 0.4, 0.6, 0.8, and 1.0, respectively, to observe the change in the probability distribution curve for v_L. All curves intersect at points *a* and *b* (Fig. 4D), and their corresponding *x* values represent two solutions for the equation $P(v_{s1}) + P(v_{r1}) + P(v_{r0}) = 0$. Because the number of bins (k) in a certain liftoff speed v_L range (we take $k = 8$ for example in Figure 4C) affects the corresponding fitting parameter values in equation 8, the values of *a* and *b* on the *x*-axis are also influenced by *k*. However, the value of *b*–*a* on the *x*-axis seems to be independent of *k*, and is roughly constant at 0.5174 m s^{-1}. In addition, we found that *a* was very close to $\bar{v}_{s1}$ and *b* was between $\bar{v}_{r0}$ and $\bar{v}_{r1}$.

Figure 4D show that when particle liftoff is only generated by collision events with $N_s = 0$ or 1, then as $p(N_s = 1)$ increases, the curve gradually develops a concave-up section between *a* and *b*, and the peak gradually moves to the left. When $p(N_s = 1) = 1.0$, an obvious bimodal distribution appears. The small changes of the probability distribution curve between *a* and *b* have been ignored in previous curve fitting. Therefore, the different shapes of the probability distribution curve for v_L (White & Schulz, 1977; Dong et al., 2002; Xie & Zheng, 2003;Cheng et al., 2006; Ho et al., 2012; Jiang et al., 2022) may only reflect a certain stage of the development of the wind–sand flow.

4. Conclusion

In our wind tunnel experiment, we used natural sand and artificial quartz sand ranging from 0.1 to 0.8 mm in diameter to study the effects of particle–bed collisions. We found an impact angle of 10.5±4.5° (mean ± SD). We found the following novel results:

N_s, v_r, and v_s were relatively independent of particle size and wind strength, but were sensitive to v_i. N_s increased linearly with increasing v_i, whereas *CoR* decreased linearly with increasing v_i, and we were able to identify a critical impact velocity required to splash particles.

The loss of momentum through frictional processes (α_{lost}) was relatively independent of v_i and remained roughly constant. Based on the assumption of conservation of momentum during collisions, we estimated a maximum value of the mean splash speed $\bar{v}_s$, which differed above and below a v_i of 7.0 m s^{-1}. Below this velocity, $\bar{v}_s$ increased approximately linearly with increasing v_i until it approached this maximum value. In contrast, above this v_i value, $\bar{v}_s$ decreased with increasing v_i and gradually became constant.

Our calculation of the probability distributions of v_L suggests that the distributions in previous research may only reflect a certain stage of the wind–sand flow.

Acknowledgments:

We gratefully acknowledge funding from the National Natural Science Foundation of China (41901012); the Open Project funding from the Key Laboratory of Desert and Desertification, Chinese Academy of Sciences (KLDD-2021-005); the Scientific Research Program Funded by Shaanxi Provincial Education Department (21JP040, 22JS017); and the China Postdoctoral Science Foundation (2019M663615). We thank Eric Parteli for fruitful discussion the physics of particle collisions, and Drs. Wanyin Luo, Guangqiang Qian, and Junfeng Lu from the Key Laboratory of Desert and Desertification, Northwest Institute of Eco-environment and Resources, Chinese Academy of Sciences, for assisting in the wind tunnel experiment.

Data Availability Statement

The data used in this analysis are archived at https://doi.org/10.5281/zenodo.7451128

References

Anderson, R. S., & Haff, P. K. (1988). Simulation of eolian saltation. *Science, 241*(4867), 820-823.

Anderson, R. S., & Haff, P. K. (1991). Wind modification and bed response during saltation of sand in air. *Acta Mechanica*, *1*, 21-51.

Bagnold, R. A. (1941). The Physics of Blown Sand and Sand Dunes. William Morrow, New York.

Beladjine, D., Ammi, M., Oger, L., & Valance, A. (2007). Collision process between an incident bead and a three-dimensional granular packing. *Physical Review E, 75*(6), 061305. https://doi.org/10.1103/PhysRevE.75.061305

Chen, Y., Zhang, J., Huang, N., & Xu, B. (2019). An experimental study on splash functions of natural sand–bed collision. *Journal of Geophysical Research: Atmospheres 121(14)*, 7226-7235.

Cheng, H., Zou, X. Y. & Zhang, C. L. (2006). Probability distribution functions for the initial liftoff velocities of saltating sand grains in air. *Journal of Geophysical Research, 111*, D22205.

Chepil, W. S. (1945). Dynamics of wind erosion. Nature of soil movement by wind. *Soil Science, 60*, 305-320.

Dong, Z. B., Liu, X. P., Li, F., Wang, H. T., & Zhao, A. G. (2002). Impact–entrainment relationship in a saltating cloud. *Earth Surface Processes and Landforms*, *27*(6), 641–658. https://doi.org/10.1002/esp.341

Gordon, M., & McKenna Neuman, C. (2009). A comparison of collisions of saltating grains with loose and consolidated silt surfaces. *Journal of Geophysical Resear*ch, 114(F4), F04015.

Ho, T.D., Valance, A., Dupont, P., & Ould El Moctar, A. (2011). Scaling law in aeolian sand transport. *Physical Review Letters, 106*, 094501.

Jiang, C.W., Parteli, E. J., Dong Z.B., Zhang, Z. C., Qian, G. Q., Luo,W. Y., Lu, J.F.,

Xiao, F. J., & Mei, F. M. (2022). Wind-tunnel experiments of aeolian sand transport reveal a bimodal probability distribution function for the particle lift-off velocities. *Catena, 217*, 106496

Kok, J. F., & Renno, N. O. (2009). A comprehensive numerical model of steady state saltation (COMSALT). *Journal of Geophysical Research: Atmospheres, 114,* D17204, doi:10.1029/2009JD011702.

Mitha, S., Tran, M. Q., Werner, B. T., & Haff, P. K. (1986). The grain-bed impact process in aeolian saltation. *Acta Mechaniea*, 63(1–4), 267–278.

McKenna Neuman, C., & Nickling, W. G. (1994). Momentum extraction with saltation. Implications for experimental evaluation of wind profile parameters. *Boundary-Layer Meteorology*, 68, 35–50.

Owen, P. R. (1964). Saltation of uniform grains in air. *Journal of Fluid Mechanics*, 20, 225–242.

Rioual, F., Valance, A., & Bideau, D. (2000). Experimental study of the collision process of a grain on a two-dimensional granular bed. *Physical Review E*, 62(2), 2450–2459. https://doi.org/10.1103/PhysRevE.62.2450

Rioual, F., Valance, A., & Bideau, D. (2003). Collision process of a bead on a two-dimensional bead packing: importance of the inter-granular contacts. *Europhysics Letters, 61*(2), 194–200.

Ungar, J. E., & Haff, P. K. (1987). Steady state saltation in air. *Sedimentology, 34*(2), 289–299.

White, B.R., & Schulz, J.C. (1977). Magnus effect in saltation. *Journal of Fluid Mechanics*, *81*, 497–512.

Xie, L. (2005) Theoretical study on liftoff velocity distribution and splash of sand particles based on particle-bed collision in wind-blown sand flux. Ph.D. thesis, Lanzhou University. (In Chinese)

Xie, L., & Zheng, X.J.(2003). Distribution of initial velocity of lift-off sand particles in aeolian saltation. *Journal of Desert Research, 23,* 637–641. (In Chinese)

Zhang, C., Huang, N., & Dun, H. C. (2022). Experimental study on sand/bed collision over the Gobi surface. *Journal of Geophysical Research: Atmospheres, 127*, e2021JD035766. https://doi.org/10.1029/2021JD035766

Zhou, Y. H., Li, W. Q., & Zheng, X. J. (2006). Particle dynamics method simulations of stochastic collisions of sandy grain bed with mixed size in aeolian sand saltation. *Journal of Geophysical Research: Atmospheres, 111,* D15108. https://doi.org/10.1029/2005JD006604